ABSTRACT EN-510: #HRS2022 YIA Competition - Basic Science Finalists

Friday, April 29, 2022
9:15 AM - 10:15 AM

EN-510-01

EXERCISE CAUSES ARRHYTHMOGENIC REMODELING OF INTRACELLULAR CALCIUM DYNAMICS IN PLAKOPHILIN-2 DEFICIENT HEARTS

Chantal J.M. van Opbergen BS, MS, PhD; Alison Smith; Rakesh R. Maurya; Duk Jae Kim; Alison N. Smith; Darren J. Blackwell; Jeffrey N. Johnston; Bjorn C. Knollmann MD, PhD; Marina Cerrone MD; Alicia Lundby PhD and Mario Delmar MD, PhD, FHRS

Background: Exercise training, as well as catecholaminergic stimulation, increase the incidence of arrhythmic events in patients affected with arrhythmogenic right ventricular cardiomyopathy correlated with plakophilin-2 mutations. Separate data show that reduced abundance of PKP2 leads to dysregulation of intracellular Ca^{2+} homeostasis.
Objective: Study the relation between exercise and/or catecholaminergic stimulation, $Ca^{2+}{}_i$ homeostasis and arrhythmogenesis in PKP2-deficient murine hearts.
Methods: Experiments were carried out in a murine model of PKP2 deficiency (PKP2cKO). For training, mice underwent 75 minutes of treadmill running per day, 5 days each week for six weeks. We used methods including imaging, high-resolution mass spectrometry, electrocardiography, as well as pharmacological approaches to study functional properties of cells/hearts in vitro and in vivo.
Results: In myocytes from PKP2cKO animals, training increased sarcoplasmic reticulum Ca^{2+} load, increased frequency and amplitude of spontaneous ryanodine receptor (RyR2)-mediated Ca^{2+} release events and changed the time course of sarcomeric shortening. Phosphoproteomics analysis revealed that training led to hyper-phosphorylation of phospholamban in residues 16 and 17, suggesting a catecholaminergic component. Isoproterenol-induced increase in $Ca^{2+}{}_i$ transient amplitude showed a differential response to beta-adrenergic blockade that depended on the purported ability of the blockers to reach intracellular receptors. Additional experiments showed significant reduction of ISO-induced $Ca^{2+}{}_i$ sparks and ventricular arrhythmias in PKP2cKO hearts exposed to an experimental blocker of RyR2 channels.
Conclusion: Exercise disproportionately affects $Ca^{2+}{}_i$ homeostasis in PKP2-deficient hearts, in a manner facilitated by stimulation of intracellular beta-ARs and hyper-phosphorylation of PIn. These cellular changes create a pro-arrhythmogenic state that can be mitigated by RyR2 blockade. We suggest that membrane-permeable beta-blockers are potentially more efficient for ARVC patients, highlight the potential for RyR2 channel blockers as treatment for the control of heart rhythm in the population at risk and propose that PKP2-dependent, and PIn-dependent ARVC-related arrhythmias have a common mechanism.

EN-510-02

SUPPRESSION AND REPLACEMENT GENE THERAPY FOR *KCNH2*-MEDIATED ARRHYTHMIAS

Sahej Bains BS; Wei Zhou MD; Steven Michael Dotzler BA; Katherine Martinez; Changsung John Kim PhD; David Tester BS and Michael John Ackerman MD, PhD

Background: *KCNH2*-mediated arrhythmias are caused by either loss-of-function (type 2 long QT syndrome, LQT2) or gain-of-function (type 1 short QT syndrome, SQT1) pathogenic variants in the *KCNH2*-encoded Kv11.1 potassium channel which is essential for the rapid delayed rectifier current (I_{Kr}) that contributes to the cardiac action potential (AP). No current therapies target the molecular cause of either LQT2 or SQT1.
Objective: To rescue the pathologic phenotype in cell models of LQT2 and SQT1 using our novel gene therapy.
Methods: A dual-component "suppression-and-replacement" (SupRep) *KCNH2* gene therapy was created by cloning into a single construct a custom-designed *KCNH2* shRNA that produces ~80% knockdown (suppression) and a "shRNA-immune" (shIMM) *KCNH2* cDNA (replacement). Patient-derived induced pluripotent stem cell-derived cardiomyocytes (iPSC-CMs) and their CRISPR-Cas9 variant-corrected isogenic control (IC) iPSC-CMs were made for 3 LQT2- (G604S, G628S, N633S) and 1 SQT1- (N588K) causative variants. All 4 variant lines were treated with KCNH2-SupRep or non-targeting control shRNA (sham). FluoVolt voltage dye was used to measure the APD at 90% repolarization (APD_{90}).
Results: KCNH2-SupRep achieved mutation-independent rescue of the pathologic phenotype in both LQT2 and SQT1. For LQT2-causative variants, treatment with KCNH2-SupRep resulted in shortening of the pathologically prolonged APD_{90} to near curative (IC-like) APD_{90} levels (G604S IC, 471±25ms; G628S IC, 429±16ms; N633S IC, 405±55ms) compared to treatment with sham (G604S: SupRep-treated, 452±76ms vs. sham-treated, 550±41ms, $p<0.0001$; G628S: SupRep-treated, 491±38ms vs. sham-treated, 674±20ms, $p<0.0001$; N633S: SupRep-treated, 399±105ms vs. sham-treated, 577±39ms, $p<0.0001$). Conversely, for the SQT1-causative N588K, treatment with KCNH2-SupRep resulted in therapeutic prolongation of the pathologically shortened APD_{90} (IC: 429±16ms; SupRep-treated: 396±61ms; sham-treated: 274±12ms).
Conclusion: We provide the first proof-of-principle gene therapy for correction of both LQT2 and SQT1. Akin to our sentinel discovery of SupRep gene therapy for LQT1, KCNH2-SupRep gene therapy successfully corrected/normalized the pathologic APD_{90}, thereby eliminating the pathognomonic feature of both LQT2 and SQT1.

EN-510-03

SINOATRIAL NODE DYSFUNCTION IN HEART FAILURE WITH PRESERVED EJECTION FRACTION

Thassio Mesquita PhD; Rodrigo Miguel dos Santos; Xaviar Michael Jones MD; Jacob Motawakel; Jae Hyung Cho MD, PhD; Mario Fournier; Weixin Liu; Eduardo Marban MD, PhD, FHRS and Eugenio Cingolani MD

Background: Under normal conditions, the human heart beats over 2 billion times during an average lifetime due to rhythmic electrical impulses initiated in the sinoatrial node (SAN). In disease conditions, such as heart failure with preserved ejection fraction (HFpEF), failure to maintain and regulate the heart rate due to SAN dysfunction can occur. We recently identified latent SAN dysfunction in animal models of cardiometabolic HFpEF. However, little is known about the metabolic imbalances underlying SAN dysfunction in HFpEF.
Objective: To identify metabolically-driven functional and transcriptomic changes in HFpEF SAN.
Methods: Male C57Bl6 mice fed with high fat (HFD) plus nitric oxide inhibitor (L-NAME) diet or regular chow served as HFpEF and control, respectively. RNA sequencing and optical mapping of SAN preparations from control and HFpEF-verified mice were performed.
Results: After 20 weeks of HFD+L-NAME, the sinus node recovery time was significantly prolonged in HFpEF mice compared to controls (162 $\pm$ 25 vs 88 $\pm$ 19 ms; $p<0.05$). Transcriptome profiling of SAN tissue revealed a significant enhancement of multiple disease-associated genes, with striking changes in extracellular matrix genes and metabolic pathways. In concordance with the observed fibrotic remodeling, conduction velocity (CV) was significantly lower in SAN of HFpEF mice compared to controls (6.4 $\pm$ 0.5 vs 13.1 $\pm$ 1.7 cm/s; $p<0.05$). Moreover, although β-adrenergic receptor stimulation accelerated the CV in control SAN, failed to do so in HFpEF animals (20 $\pm$ 3.1 vs 10.2 $\pm$ 1.1 cm/s; $p<0.05$).
Conclusion: Our results using a cardiometabolic HFpEF model indicate that SAN dysfunction is closely associated with molecular changes in metabolic pathways and extracellular matrix remodeling associated genes. Understanding the metabolic control of the SAN may open new therapeutic targets for HFpEF associated SAN dysfunction.

ABSTRACT EN-571:
#HRS2022 YIA Competition - Clinical EP Finalists

Friday, April 29, 2022
10:30 AM - 11:30 AM

EN-571-01

THE VALUE OF PROGRAMMED VENTRICULAR EXTRASTIMULI FROM THE RIGHT VENTRICULAR BASAL SEPTUM DURING SUPRAVENTRICULAR TACHYCARDIA

Satoshi Higuchi MD; Hiroyuki Ito MD; Edward P. Gerstenfeld MD, FHRS; Adam C. Lee MBBS, CEPS-A, CCDS; Byron K. Lee MD; Gregory M. Marcus MD, FHRS; Henry H. Hsia MD, FHRS; Joshua D. Moss MD, FHRS; Randall J. Lee MD, PhD; Thomas A. Dewland MD, FHRS; Vasanth Vedantham MD, PhD; Zian H. Tseng MD, MS; Akash R. Patel MD, FHRS, CEPS-P; Ronn E. Tanel MD, FHRS, CEPS-P; Nitish Badhwar MBBS, FHRS; Cara N. Pellegrini MD, FHRS; Mitsuharu Kawamura MD; Morio Shoda MD, PhD; Chun Hwang MD, FHRS; Marwan M. Refaat MD, FHRS and Melvin M. Scheinman MD, FHRS

Background: The difference between a right ventricular (RV) apical stimulus-atrial electrogram (SA) during reset of supraventricular tachycardia (SVT) vs. the ventriculoatrial interval during SVT ($\Delta SA\text{-}VA_{apex}$) is an established technique for discerning SVT mechanisms but is limited by significant diagnostic overlap.

Objective: We hypothesized that ΔSA-VA intervals from the RV basal septum ($\Delta SA\text{-}VA_{base}$) would be shorter than from the RV apex for atrioventricular reciprocating tachycardia (AVRT) and would show the opposite effects to that of atrioventricular nodal re-entrant tachycardia (AVNRT) (Figure 1). Moreover, it was predicted that RV basal pacing might be useful for distinguishing septal from free wall accessory pathways (APs).

Methods: In this multicenter prospective study, all AVNRT and AVRT patients underwent programmed ventricular extrastimuli (V2) delivered from both the RV basal septum and RV apex. Both the $\Delta SA\text{-}VA_{base}$ and $\Delta SA\text{-}VA_{apex}$ were calculated when V2 clearly reset the tachycardia.

Results: The V2 technique was successfully performed from both sites in 105 AVNRT (age 48±20, 44% male) and 130 AVRT (age 26±18, 54% male) patients. The $\Delta SA\text{-}VA_{base}$ was shorter than the $\Delta SA\text{-}VA_{apex}$ during AVRT (44±29 vs. 58±29ms, $p<0.001$), and the opposite occurred during AVNRT (133±31 vs. 125±25ms, $p=0.03$). A $\Delta SA\text{-}VA_{base}$ of ≧85ms had a sensitivity of 97% and specificity of 98% for identifying AVNRT (area under the receiver operating characteristic curve: 0.988, 95% confidential interval:0.974-1.000). Furthermore, a $\Delta SA\text{-}VA_{base}$ of 45-85ms allowed identifying AVRT with left free wall APs (sensitivity 88%/specificity 95%), 20-45ms for posterior septal APs (sensitivity 83%/specificity 96%), and <20ms for right free wall or anterior/mid septal APs (sensitivity 86%/specificity 99%) (Figure 2).

Conclusion: The $\Delta SA\text{-}VA_{base}$ during V2 produced a more robust differentiation between AVNRT and AVRT compared with the $\Delta SA\text{-}VA_{apex}$. The $\Delta SA\text{-}VA_{base}$ of ≧85ms proved to be excellent for the differentiation of all AVNRT from AVRT regardless of the AP location. Furthermore, this straightforward technique allowed localizing four general AP locations with a high sensitivity and specificity.

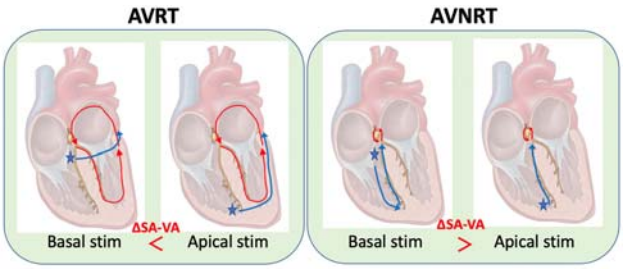

Figure 1

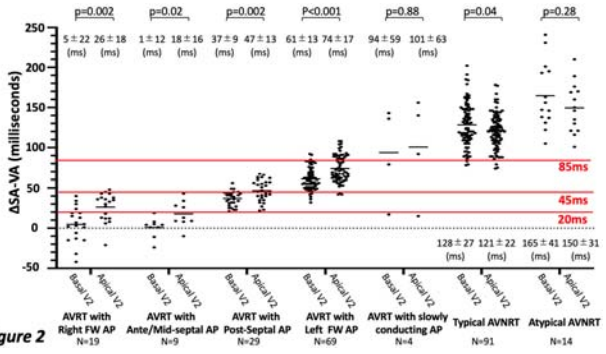

Figure 2

EN-571-02

SCREENING FOR PUTATIVE PATHOGENIC VARIANTS IN DILATED CARDIOMYOPATHY GENES IDENTIFIES EARLY DISEASE AND PREDICTS MORTALITY

Ravi Shah MB BChir; Babken Asatryan MD, PhD; Ghaith Sharaf Dabbagh MD; Mohammed Khanji; Stefan van Duijvenboden; Daniele Muser MD; Andrew Paul Landstrom MD, PhD, FHRS; Christopher Semsarian MBBS, MPH, PhD, FHRS; Virend Somers MD, PhD; Patricia B. Munroe BS, MSci, PhD and Anwar A. Chahal BS, MBChB, PhD

Background: Dilated cardiomyopathy (DCM) can present with the sentinel event of sudden cardiac death, as well as heart failure, ECG abnormalities, atrial fibrillation or stroke. Data are limited regarding genetic screening and the mortality associated with DCM in a general population.

Objective: Using the UK Biobank, we aimed to determine the mortality and clinically relevant outcomes associated with putative pathogenic variants (PuPV) in DCM genes.

Methods: Cohort study design using whole exome sequencing; variants in 44 ClinGen-curated DCM genes were annotated using REVEL (≥0.65) and ANNOVAR (predicted loss of function) to identify PuPVs and assign individuals to the genotype-positive (G+) or genotype-negative (G- [controls]) cohorts. Group comparisons were made using time-to-event analysis to investigate mortality and composite outcomes of DCM, heart failure, arrhythmia, and stroke.

Results: In 200,619 participants, PuPV in DCM genes were identified in 16,674 (8.3%) individuals (G+). G+ and G- had similar proportion of females (54.6% vs 55.1%; p=0.23). G+ participants were slightly younger (56.3 vs 56.5 years; p=0.003). Of G+, 1703 (10.2%) had subclinical DCM and 84 (0.5%) had clinical DCM . G+ had increased mortality (HR 1.08 [95% CI 1.01 - 1.15]) and increased risk of developing the composite outcomes (HR 1.11 [95% CI 1.06

- 1.17]). Age at death was not different (69.7 vs 69.7 years; p=0.75).

Conclusion: Adults with PuPV in 44 DCM genes have higher all-cause mortality and increased risk of developing DCM-associated features and complications, compared to G- controls.

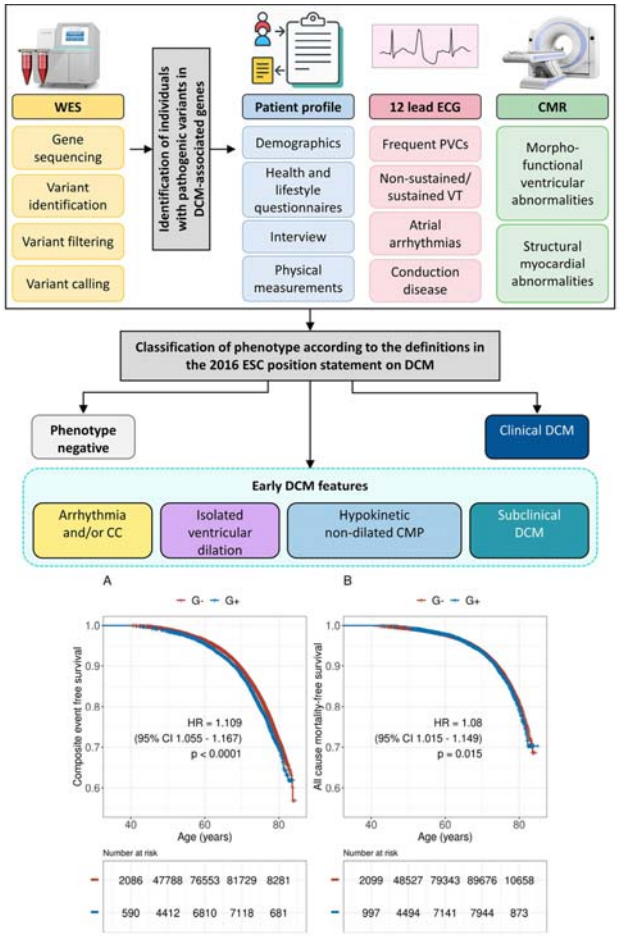

EN-571-03

RISK STRATIFICATION OF PATIENTS WITH BRUGADA SYNDROME BY NON-INVASIVE HIGH DENSITY ELECTROCARDIOGRAFIC MAPPING SYSTEM

Cinzia Monaco; Luigi Pannone; Juan Antonio Sieira Rodriguez - Moret; Vincenzo Miraglia; Antonio Bisignani; Gian Battista Chierchia and Carlo de Asmundis MD, PhD, FHRS

Background: Risk stratification in patients affected by Brugada syndrome is a crucial moment for the therapeutic management, as this pathology is increasingly diagnosed in young subjects without further comorbidities.
Objective: To provide a risk stratification in patients affected by Brugada syndrome that can relies on clinical and electrophysiological data at the same time.
Methods: We reported our single-Centre experience from January 2016 to October 2021; all consecutive patients with Brugada Syndrome undergoing non-invasive high-density electrocardiographic mapping were included in the study. We defined the correlation between the clinical risk factors and the extension of the pathological substrate in patients with Brugada syndrome analyzed by non-invasive high density electrocardiographic mapping system and a new generation software developed for the post-processing analysis.
Results: In patients with spontaneous Brugada type 1 ECG pattern, the pathological substrate areas were always larger than the patients without spontaneous pattern; the results were statistically significant during stress test (3±3,75 vs 15,57±11,16; p=0,00024) and after Ajmaline administration (12,61±11,3 vs 25,74±20,02; p=0,04). In patients with familiarity for first-degree relatives SCD before 35 y.o. the areas were on average wider, in the baseline this difference was statistically relevant (3,6±5,46 vs 10,33±10,51; p=0,03). In patients with aborted SCD the average of the areas was always larger than in patients who did not present this risk factor, with statistically significant results at baseline (4,76±6,75 vs 17,29±13,58; p=0,04) and after pharmacological induction with Ajmaline (11,61±10,04 vs 35,49±17,23; p=0,0003).
Conclusion: Latest generation technologies such as non-invasive high-density electrocardiographic mapping systems can represent a new frontier in the study of BrS patients, through the identification and measurement of pathological areas and their correlation with the patient's clinical history and risk factors; moreover, this technology provide a valuable aid in the pre-procedural study of high-risk patients by identifying the pathological areas that will be subject to ablation.